Dissociation dynamics of ion-pair states of Cl_2 at principal quantum numbers beyond 1500

Sandro Mollet and Frédéric Merkt
Laboratorium für Physikalische Chemie, ETH Zürich,CH-8093 Zürich, Switzerland
(Received 16 July 2010; published 23 September 2010)

Long-lived ion-pair states of Cl_2 have been observed by delayed pulsed-field ionization in the vicinity of the $Cl^-(^1S_0) + Cl^+(^3P_2)$ dissociation threshold following single-photon excitation from the $X\ ^1\Sigma_g^+(v = 0)$ ground state with a tunable vacuum-ultraviolet laser. The field-ionization spectra reveal a series of resonances corresponding to ion-pair states with effective principal quantum number n^* between 1858 and 1876 belonging to a series converging to the $Cl^-(^1S_0) + Cl^+(^3P_0)$ dissociation threshold. These states are observed by forced predissociation into the $Cl^-(^1S_0) + Cl^+(^3P_2)$ ion-pair channel. This process is the ion-pair analog of the process of forced autoionization observed in Rydberg states. The analysis of the spectra and of the field-ionization behavior provides information on the couplings between the relevant ionization and dissociation channels and has enabled the determination of the ion-pair dissociation threshold [$E_{IPD}(Cl^-(^1S_0) + Cl^+(^3P_2)) = 95\,449.8 \pm 1.0\,cm^{-1}$] and of the dissociation energies of Cl_2 [$D_0(X\ ^1\Sigma_g^+) = 19\,998.4 \pm 1.1\,cm^{-1}$] and Cl_2^+ [$D_0(X^+\ ^2\Pi_u) = 31\,942.1 \pm 1.5\,cm^{-1}$].

DOI: 10.1103/PhysRevA.82.032510 PACS number(s): 33.15.Ry, 32.80.Ee, 33.20.Ni

I. INTRODUCTION

Ion-pair states are vibrational levels associated with the attractive $-1/r$ potential binding two ions of opposite charge. They are qualitatively analogous to Rydberg states, the anion replacing the electron. Their spectral positions can be described by Rydberg's formula:

$$\tilde{\nu} = \frac{E_{IPD}}{hc} - \frac{R_{Cl^+-Cl^-}}{(n-\delta)^2} = \frac{E_{IPD}}{hc} - \frac{R_{Cl^+-Cl^-}}{n^{*2}}, \qquad (1)$$

where E_{IPD} is the ion-pair dissociation energy, $R_{Cl^+-Cl^-}$ the Rydberg constant of the ion-pair system, n the principal quantum number, δ the quantum defect, and n^* the effective principal quantum number. However, significant quantitative differences from the behavior of Rydberg states result from the very different reduced masses, which is the reason why these states are also referred to as heavy Rydberg states [1]. In the case of ion-pair states of $^{35}Cl_2$, the reduced mass [$M = (\mu_{^{35}Cl^+-^{35}Cl^-})/m_e$] is 31 872.16 times larger than for a Rydberg state so that the Rydberg constant ($R_{^{35}Cl^+-^{35}Cl^-} = R_\infty M$) is $3.4976 \times 10^9\,cm^{-1}$ and the Bohr radius [$a_{0,^{35}Cl^+-^{35}Cl^-} = a_0(1/M)$] is 1.66×10^{-15} m, that is, smaller than a Cl nucleus. The principal quantum number n of an ion-pair state is given by $v + J + 1$, where v and J are the vibrational and rotational quantum numbers [2]. Table I compares the properties of an ion-pair state of Cl_2 with principal quantum number $n = 1000$ to those of a Rydberg state of H of the same principal quantum number (first two columns) and of the same binding energy $E_b/hc = 10\,cm^{-1}$ (last two columns).

Ion-pair states of high principal quantum number have received attention recently in the context of the spectroscopic technique called threshold ion-pair production spectroscopy (TIPPS) [3–5] and also in relation to fundamental aspects of so-called heavy Rydberg systems [1,6–9]. Predissociative ion-pair states of a molecule AB (where A and B can be atoms or molecules) are observable in photoionization spectra by monitoring either the positively (A^+) or the negatively (B^-) charged fragment. In such spectra, the positively charged fragment (A^+) can be observed at energies below the dissociative ionization threshold of the molecular cation ($AB \rightarrow A^+ + B$) if fragment B has a positive electron affinity [10].

The precise determination of ion-pair dissociation thresholds (E_{IPD}) can be exploited to derive electron affinities (E_A), bond dissociation energies (D_0), or ionization energies (E_I) using thermochemical cycles, as given in Eqs. (2) and (3) [11]:

$$E_{IPD} = D_0(AB) + E_I(A) - E_A(B), \qquad (2)$$

$$E_{IPD} = D_0(AB^+) + E_I(AB) - E_A(B). \qquad (3)$$

The observation of ion-pair states of high principal quantum number by direct photoexcitation from the ground state is usually hindered by extremely small Franck-Condon factors and is intrinsically linked to complex interactions between dissociation and ionization channels at short internuclear distances [1–3,10,12–14]. So far, interactions between series of ion-pair states converging to different ion-pair dissociation thresholds have neither been observed nor discussed in the literature, presumably because the amplitudes of ion-pair wave functions are very small at short internuclear distances, where the channel interactions take place. We report here on the observation of ion-pair states of Cl_2 which reveal the existence of such interactions.

Cl_2 is an ideal system to study ion-pair states [11–19] because the very large electron affinity of the Cl atom makes it possible to observe these states over a wide energy range below the first dissociative ionization threshold. Moreover, Cl^+ possesses several low-lying electronic states, which offers the possibility, exploited in the present study, of studying interactions between different series of ion-pair states.

The position of the $Cl^-(^1S_0) + Cl^+(^1D_2) \leftarrow Cl_2(X\ ^1\Sigma_g^+)$ ion-pair dissociation threshold has been measured to be $107\,096^{+8}_{-2}\,cm^{-1}$ by Li *et al.* [17] using imaging of the charged fragments emitted in the continuum above the ion-pair dissociation threshold. Zhou, Hao and Mo have also studied the ion-pair dissociation dynamics over a wide energy range above the lowest ion-pair dissociation threshold [18,19]. Compared to imaging studies of ion-pair dissociation continua, field ionization studies of bound ion-pair levels offer the advantages of being more precise and of providing additional,

TABLE I. Comparison of Rydberg state and ion-pair state properties. The left two columns compare states with identical principal quantum number $n = 1000$ but different binding energies, and the right two columns compare states with identical binding energies $E_b/hc = 10\,\mathrm{cm}^{-1}$.

	$n = 1000$		$E_b/hc = 10\,\mathrm{cm}^{-1}$	
	$H^+ - e^-$	$Cl^+ - Cl^-$	$H^+ - e^-$	$Cl^+ - Cl^-$
$r_{\mathrm{classical}}$	53 μm	1.7 nm	5.5 nm	581 nm
$E_b/hc; n$	0.1 cm^{-1};–	3500 cm^{-1};–	–; 105	–; 18 700
$\Delta E_{n,n+1}/hc$	0.0002 cm^{-1}	7 cm^{-1}	0.2 cm^{-1}	0.001 cm^{-1}
$F_{\mathrm{ion,classical}}$	0.3 mV/cm	330 kV/cm	2.7 V/cm	2.7 V/cm
$F_{\mathrm{Inglis\text{-}Teller}}$	1.7 μV/cm	1.7 kV/cm	0.14 V/cm	0.76 mV/cm

complementary information on the ion-pair levels, as will be shown subsequently.

II. EXPERIMENTAL

The experiments were carried out using the tunable vacuum-ultraviolet (VUV) laser system described in Ref. [20]. Tunable VUV radiation with a bandwidth of $\approx$0.5 cm^{-1} was generated by resonance-enhanced sum-frequency mixing $\tilde{\nu}_{\mathrm{VUV}} = 2\tilde{\nu}_1 + \tilde{\nu}_2$ in Xe using the $(5p)^5 6p[1/2]_0 \leftarrow (5p)^6\ ^1S_0$ two-photon resonance at $2\tilde{\nu}_1 = 80\,118.984\,\mathrm{cm}^{-1}$. The spectra were acquired by monitoring the yields of threshold photoelectrons and of Cl^-, Cl^+, and Cl_2^+ ions using a time-of-flight mass spectrometer. Prompt Cl^- and Cl^+ ions produced by photoionization were separated from Cl^- and Cl^+ ions produced by delayed pulsed-field dissociation (PFD) by applying a weak dc field using a method closely related to mass-analyzed-threshold-ionization spectroscopy [21]. The threshold ion-pair dissociation spectra were recorded using TIPPS, as described in Refs. [3–5]. The Cl_2 sample was introduced into the spectrometer using a pulsed valve producing a supersonic expansion. A gas mixture of Ar and Cl_2 with a pressure ratio of 10:1 was used at a stagnation pressure of 1.5 bar. The supersonic expansion was skimmed and crossed the VUV laser beam at right angles in the middle of a cylindrical electrode stack used to extract the charged particles toward a microchannel plate detector by applying continuous and pulsed electric fields. The spectra were obtained by monitoring the corresponding ion or electron currents as a function of the VUV laser wave number.

III. RESULTS

The spectra in Figs. 1(a) and 1(b) display the yield of $^{35}Cl^+$ and $^{35}Cl^-$ ions obtained by delayed PFD of long-lived ion-pair states located below the $Cl^-(^1S_0) + Cl^+(^3P_2)$ dissociation threshold. The former was recorded using a pulsed field of 460 V cm^{-1} applied 12 μs after photoexcitation, whereas the latter was obtained by applying a pulsed field of -100 V cm^{-1} 10 μs after photoexcitation. The two spectra are almost identical. They each consist of two broad resonances indicated by dashed lines, on which a series of sharper resonances is superimposed. The spectrum in Fig. 1(c) displays the $^{35}Cl^+$ signal recorded using a much smaller pulsed electric field of 3 V cm^{-1}, and the spectra in Figs. 1(d) and 1(e) correspond to the prompt $^{35}Cl^+$ ion signal and the $^{35}Cl_2^+$ photoionization signal, respectively. In Fig. 1(d), two traces are plotted, one observed by extracting the prompt $^{35}Cl^+$ ion signal with a dc field of 3 V cm^{-1} (solid line), the other with a dc field

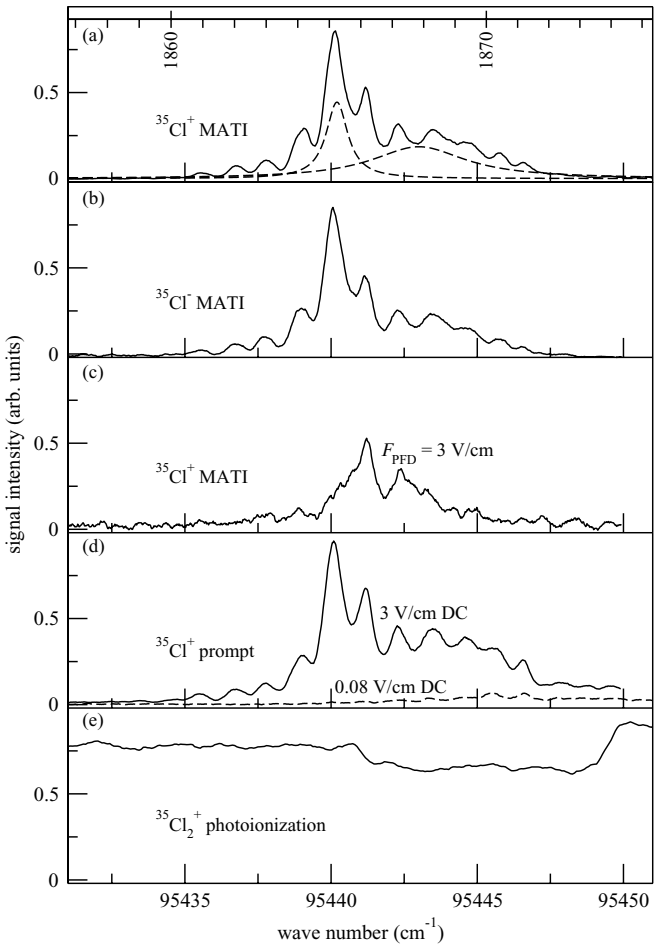

FIG. 1. Spectra recorded in the region of the $Cl^-(^1S_0) + Cl^+(^3P_2)$ ion-pair dissociation threshold. (a) $^{35}Cl^+$ ion signal produced by a delayed pulsed electric field of 460 V cm^{-1} in the presence of a weak dc electric field of 0.08 V cm^{-1}. The dashed lines indicate the estimated positions and widths of the two Rydberg states of Cl_2, which carry the spectral intensity in this region. (b) $^{35}Cl^-$ ion signal produced by a pulsed electric field of -100 V cm^{-1}. (c) $^{35}Cl^+$ ion signal produced by a pulsed electric field of 3 V cm^{-1}. (d) Prompt $^{35}Cl^+$ ion signal extracted by dc electric fields of 3 V cm^{-1} (solid line) and 0.08 V cm^{-1} (dashed line). (e) $^{35}Cl_2^+$ photoionization yield. The top assignment bar indicates the effective principal quantum number n^*.

of only $0.08\,\mathrm{V\,cm^{-1}}$ (dashed line). Several conclusions can immediately be drawn by comparison of these spectra:

(a) The almost identical appearance of the $^{35}Cl^+$ and $^{35}Cl^-$ ion yields in Figs. 1(a) and 1(b) strongly suggests that both types of ions are produced by the same mechanism. The ions are produced by the pulsed field, from which one must conclude that this mechanism is delayed PFD of highly excited ion-pair states, the equivalent of delayed pulsed-field ionization in Rydberg states.

(b) The blue shift in the low–wave-number onset of the $^{35}Cl^+$ signal observed when the pulsed electric field is reduced from $460\,\mathrm{V\,cm^{-1}}$ [Fig. 1(a)] to $3\,\mathrm{V\,cm^{-1}}$ [Fig. 1(c)] actually proves that the signal originates from delayed PFD. Assuming that the dissociation occurs diabatically (in analogy to the field ionization of high Rydberg states [22]), the low-frequency onset of the $^{35}Cl^+$ peak in Fig. 1(c) would be expected to be observed at

$$\frac{\Delta E}{hc\,\mathrm{cm^{-1}}} = 4\sqrt{F/(\mathrm{V\,cm^{-1}})} \tag{4}$$

below the field-free dissociation threshold, which would imply a field-free dissociation threshold of about $95\,448\,\mathrm{cm^{-1}}$. A more systematic way of determining the position of this threshold will be described later.

(c) The prompt $^{35}Cl^+$ signal and its strong dependence on the value of the dc electric field [see Fig. 1(d)] can also be interpreted as a lowering of the dissociation threshold by the electric field and enable one to rule out the dissociation of Cl_2 into two neutral Cl fragments followed by the ionization of one of the fragments as a significant source of Cl^+ signal. Indeed, no mechanism can be thought of by which this process would be so strongly dependent on the value of the dc electric field.

(d) The Cl_2^+ signal [cf. Fig. 1(e)] does not vary sharply over the wave number range of the figure, which indicates that the states that give rise to the Cl^+ and Cl^- dissociation products are not coupled to a Cl_2^+ ionization continuum.

(e) The width of more than $0.5\,\mathrm{cm^{-1}}$ of the resonances observed in the $^{35}Cl^+$ and $^{35}Cl^-$ spectra does not reflect the lifetimes of the ion-pair states detected by delayed PFD because the field dissociation pulse was applied more than 5μs after photoexcitation, and a width of $0.5\,\mathrm{cm^{-1}}$ would correspond to a lifetime of ≈10 ps. The observed width of $\approx 0.5\ \mathrm{cm^{-1}}$ thus represents an upper bound to the coupling strength of the $Cl^-(^1S_0) + Cl^+(^3P_0)$ ion-pair states with $n^* \approx 1800$ to the pseudocontinuum of very high ion-pair states located below the $Cl^-(^1S_0) + Cl^+(^3P_2)$ dissociation limit (see Fig. 4).

To determine a more precise value of the field-free dissociation threshold, a series of PFD spectra were recorded using a delayed pulsed electric field of $50\,\mathrm{V\,cm^{-1}}$ and by carrying out the photoexcitation in the presence of dc electric fields of different strengths. The effect of these electric fields is to prevent the observation of the highest ion-pair states and to induce a shift,

$$\frac{\Delta E}{hc\,\mathrm{cm^{-1}}} = -c\sqrt{F/(\mathrm{V\,cm^{-1}})}, \tag{5}$$

of the high–wave-number edge of the PFD signal, with $c \approx 6$. The reason for the disappearance of the highest ion-pair states is that a homogeneous electric field distorts the unperturbed Coulomb potential in such a way that a saddle point arises in the potential surface, and all states lying above the saddle point energy field dissociate. This situation is analogous to that encountered in electronic Rydberg states. In the limiting case of static electric fields and purely classical field dissociation (or field ionization), the constant c would take the value 6.12.

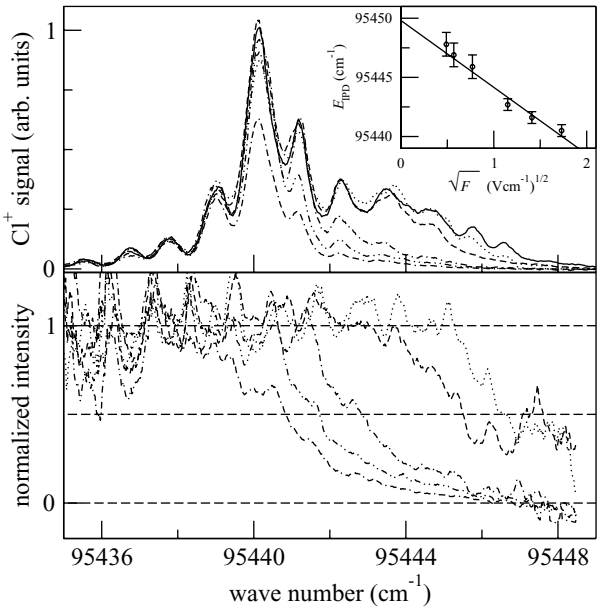

FIG. 2. (top) $^{35}Cl^+$ ion signal produced by the pulsed electric field in the presence of dc offset fields of $0.08\,\mathrm{V\,cm^{-1}}$ (solid line), $0.33\,\mathrm{V\,cm^{-1}}$ (dotted line), $0.59\,\mathrm{V\,cm^{-1}}$ (dashed line), $1.32\,\mathrm{V\,cm^{-1}}$ (dash-dotted line), $2\,\mathrm{V\,cm^{-1}}$ (dash-double-dotted line), and $3\,\mathrm{V\,cm^{-1}}$ (dotted-double-dashed line). (bottom) Spectra of (top), normalized to the intensity of the spectrum recorded with the smallest dc field. Inset shows the determination of the field-free $Cl^-(^1S_0) + Cl^+(^3P_2)$ ion-pair dissociation threshold by linear regression. The graph was obtained by plotting the wave number at which the normalized intensity is 0.5 as a function of the square root of the dc field strength.

The traces displayed in Fig. 2 (top) show the PFD signal observed in the presence of dc fields of varying strength. Normalizing the spectra to the intensity of the spectrum recorded with the smallest dc field leads to the series of field dissociation yields depicted in Fig. 2 (bottom), which enables one to clearly recognize the gradual shifts of the high–wave-number edge of the PFD spectra with increasing dc field strength.

Analyzing the positions where the normalized field-dissociation signals have reached half of their maximal value with Eq. (5) leads to a field-free $Cl^-(^1S_0) + Cl^+(^3P_2) \leftarrow Cl_2(X\,^1\Sigma_g^+)$ ion-pair dissociation threshold of $95\,449.8 \pm 1.0\,\mathrm{cm^{-1}}$ and a value of c of 5.7 ± 0.4, as illustrated by the linear regression presented in the inset in Fig. 2. Using this value of the $Cl^-(^1S_0) + Cl^+(^3P_2)$ ion-pair dissociation threshold in combination with the known term values of Cl^+ [$\tilde{\nu}(^3P_2) = 0\,\mathrm{cm^{-1}}$, $\tilde{\nu}(^3P_1) = 696.00\,\mathrm{cm^{-1}}$, $\tilde{\nu}(^3P_2) = 996.47\,\mathrm{cm^{-1}}$, $\tilde{\nu}(^1D_2) = 11\,653.58\,\mathrm{cm^{-1}}$, $\tilde{\nu}(^1S_0) = 27\,878.02\,\mathrm{cm^{-1}}$] [23], all low-lying ion-pair dissociation

thresholds of Cl_2 can be determined as follows:

$$E_{\mathrm{IPD}}(\mathrm{Cl}^-(^1S_0)+\mathrm{Cl}^+(^3P_2)) = 95\,449.8 \pm 1.0\,\mathrm{cm}^{-1}, \quad (6a)$$

$$E_{\mathrm{IPD}}(\mathrm{Cl}^-(^1S_0)+\mathrm{Cl}^+(^3P_1)) = 96\,145.8 \pm 1.0\,\mathrm{cm}^{-1}, \quad (6b)$$

$$E_{\mathrm{IPD}}(\mathrm{Cl}^-(^1S_0)+\mathrm{Cl}^+(^3P_0)) = 96\,446.3 \pm 1.0\,\mathrm{cm}^{-1}, \quad (6c)$$

$$E_{\mathrm{IPD}}(\mathrm{Cl}^-(^1S_0)+\mathrm{Cl}^+(^1D_2)) = 107\,103.4 \pm 1.0\,\mathrm{cm}^{-1}, \quad (6d)$$

$$E_{\mathrm{IPD}}(\mathrm{Cl}^-(^1S_0)+\mathrm{Cl}^+(^1S_0)) = 123\,327.8 \pm 1.0\,\mathrm{cm}^{-1}. \quad (6e)$$

The series of resonances observed below the $Cl^-(^1S_0)+Cl^+(^3P_2)$ ion-pair dissociation threshold does not correspond to the ion-pair states converging to this limit because the principal quantum numbers of ion-pair states of Cl_2 having binding energies of less than $20\,\mathrm{cm}^{-1}$ exceed 13 000, and the spacing of $\Delta E/hc < 0.003\,\mathrm{cm}^{-1}$ between adjacent members of the series is much smaller than the spacing of $\Delta E/hc \approx 1.075\,\mathrm{cm}^{-1}$ between the members of the series observed in Fig. 1.

The series cannot be attributed to a normal Rydberg series converging to vibrationally excited states of the $X^+\,^2\Pi_g$ electronic ground state of Cl_2^+ either, nor to one converging to an electronically excited state of the ion, because the spacings between neighboring states of a Rydberg series would not remain almost constant over the energy range of Fig. 1. The observed pattern does not originate from the rotational structure of a vibronic band either because the rotational constant of Cl_2 is far too small (on the order of $0.25\,\mathrm{cm}^{-1}$ [24]), and the rotational temperature (on the order of 10 K) is far too low, to explain the observed series. We conclude that the series observed in Fig. 1 corresponds to highly excited ion-pair levels converging to a higher-lying ion-pair dissociation threshold of Cl_2, which predissociate into the pseudocontinuum of very high ($n > 13000$) vibrational levels of the $Cl^-(^1S_0)+Cl^+(^3P_2)$ ion-pair channel. Their detection is then made possible by the application of a pulsed electric field which lowers the $Cl^-(^1S_0)+Cl^+(^3P_2)$ dissociation threshold. This process is analogous to that of forced autoionization in Rydberg states [25,26], which plays an important role in pulsed-field ionization zero-kinetic-energy photoelectron spectroscopy [27,28].

The observed spacing of $\Delta E/hc = 1.075\,\mathrm{cm}^{-1}$ between neighboring members of the series enables one to estimate the effective principal quantum number of the ion-pair states to be $n^* \approx 1870$ using $\Delta E = 2R_{^{35}\mathrm{Cl}^+-^{35}\mathrm{Cl}^-}/n^{*3}$, which, in turn, indicates that the convergence limit of the series of ion-pair states is located at a position of $\approx 96\,445\ \mathrm{cm}^{-1}$. From Eqs. (6), we conclude that the corresponding ion-pair dissociation threshold must be $Cl^-(^1S_0)+Cl^+(^3P_0)$. Using this threshold, one can assign effective principal quantum numbers 1858–1876 to the observed resonances, as indicated along the assignment bars in Figs. 1(a) and 3. Whereas the positions of the predissociative resonances are reproduced satisfactorily by Eq. (1), perturbations of the series near the center of the two broad resonances indicated by dashed lines in Fig. 1(a) are noticeable. These perturbations are revealed by slight shifts of the peak maxima and gradual changes of the line profiles, as often encountered in situations where several channels interact [29,30].

To confirm this assignment, dc electric fields of increasing strength were applied until the Stark manifolds corresponding to neighboring members of the series started overlapping,

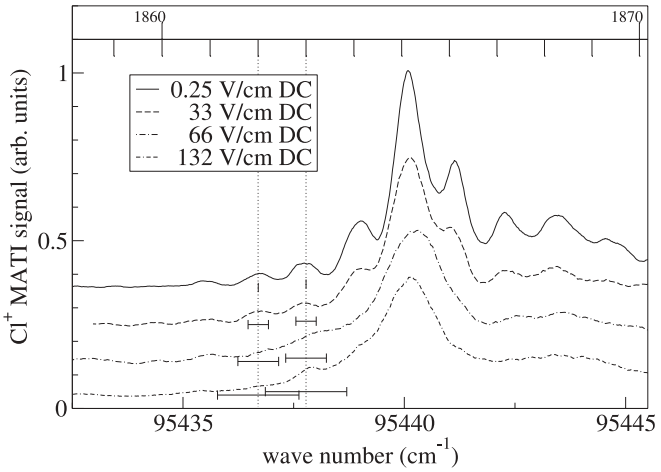

FIG. 3. $^{35}Cl^+$ ion signal produced by the pulsed electric field in the presence of different dc electric fields. The spectra have been shifted along the vertical axis for better visibility. The Inglis-Teller field F_{IT} in this region of principal quantum numbers is ≈77 V/cm. The horizontal bars indicate the width of the $n^* = 1862$ and $n^* = 1863$ Stark manifolds at the respective electric field strengths.

leading to a disappearance of the regular series (cf. Fig. 3). At this point, the electric field strength should correspond approximately to the Inglis-Teller field, which is given, in atomic units, by

$$F_{\mathrm{IT}} \approx \frac{1}{3n^{*5}} M^2. \quad (7)$$

To obtain the corresponding electric field strength in V/cm, Eq. (7) has to be multiplied by the atomic unit of electric field strength, yielding $F_{\mathrm{IT}(n^*_{\mathrm{ion-pair}}=1865)} \approx 77\,\mathrm{V/cm}$. The resonances observed at zero field in Fig. 3 start disappearing at an electric field of ≈66 V/cm, which corresponds closely to F_{IT} calculated for the effective principal quantum number $n^* = 1865$. The expected widths of the Stark manifolds corresponding to the $n^* = 1862$ and $n^* = 1863$ ion-pair states are indicated as horizontal bars below the respective traces in Fig. 3.

Figure 4 (top) summarizes the mechanism we propose to interpret the spectral stuctures observed in Fig. 1. Excitation from the vibronic ground state of Cl_2 takes place to two low-lying Rydberg states [indicated by dashed lines in Fig. 1(a)] of Cl_2, labeled $n_1(v_1^+, J_1^+)$ and $n_2(v_2^+, J_2^+)$, converging to an electronically excited state of Cl_2^+. These states lie immediately below the $Cl^-(^1S_0)+Cl^+(^3P_2)$ ion-pair dissociation threshold and above many ionization and dissociation thresholds of Cl_2. They could therefore decay into many open channels, their decay width Γ_{tot} being

$$\Gamma_{\mathrm{tot}} = \Gamma_{\mathrm{ion}} + \Gamma_{\mathrm{pred}} + \Gamma_{\mathrm{ion\text{-}pair}} + \Gamma_{\mathrm{rad}}, \quad (8)$$

where Γ_{ion}, Γ_{pred}, $\Gamma_{\mathrm{ion\text{-}pair}}$, and Γ_{rad} represent the decay widths associated with autoionization, predissociation into neutral fragments, predissociation into Cl^+ and Cl^-, and radiative decay, respectively.

The results depicted in Fig. 1 enable one to determine the dominant channel interactions. Because the Cl_2^+ ion yield remains approximately constant, we conclude that the coupling of the two Rydberg states to open ionization channels is not

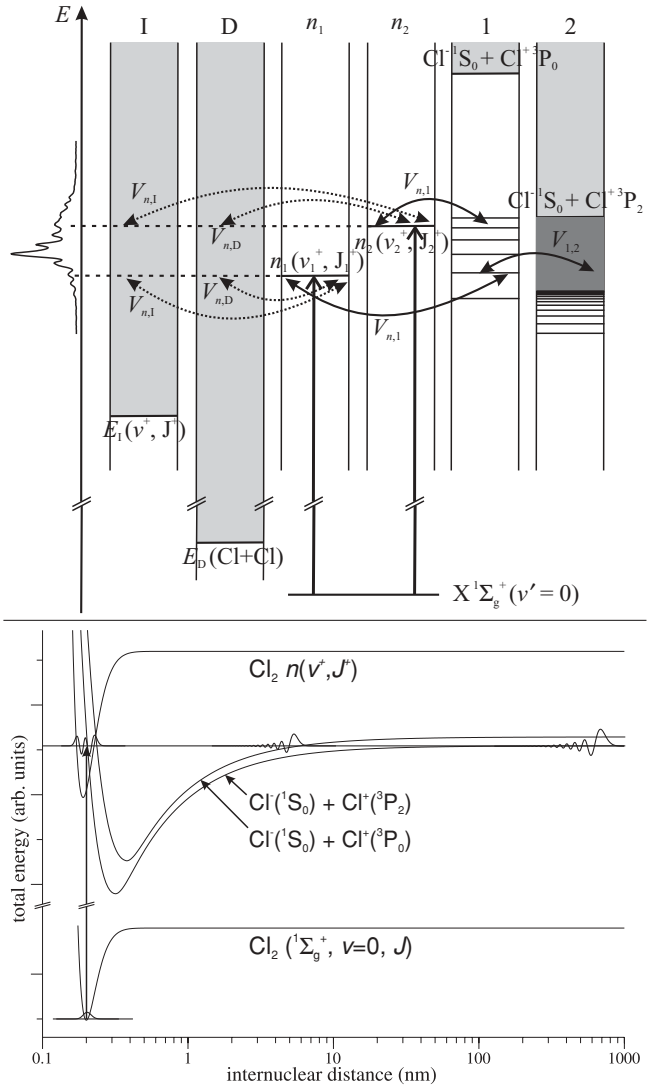

FIG. 4. (top) Schematic illustrating the mechanism proposed to explain the observed spectral structures in the vicinity of the $Cl^-(^1S_0) + Cl^+(^3P_2)$ ion-pair dissociation threshold of Cl_2. The full arrows indicate the dominant channel interactions, whereas the dotted arrows indicate interactions that appear negligible. (bottom) Schematic and qualitative illustration of the potential curves of the states involved in the proposed mechanism.

dominant. Similarly, the absence of a measurable Cl^+ ion signal from the predissociation into two neutral Cl atoms followed by photoionization of one fragment suggests that the decay into neutral dissociation channels is not important. Radiative decay cannot explain the width of $\approx 1\,cm^{-1}$ and $\approx 4\,cm^{-1}$ of the two resonances so that the interaction with ion-pair channels must be the dominant interaction for both states. The appearance of the spectrum suggests the following hierarchy of interactions: The strongest interaction $V_{n_i,I}$ is with the $Cl^-(^1S_0) + Cl^+(^3P_0)$ ion-pair channel, giving rise to the overall spectral structure; a weaker interaction $V_{I,II} < 0.5\,cm^{-1}$ between the $Cl^-(^1S_0) + Cl^+(^3P_0)$ and the $Cl^-(^1S_0) + Cl^+(^3P_2)$ channels leads to the observation of the PFD signal. The couplings $V_{n_i,ion}$ and $V_{n_i,pred}$ to the ionization and neutral dissociation channels, respectively, are too small to be observed.

That the ion-pair states associated with the $Cl^-(^1S_0) + Cl^+(^3P_0)$ and $Cl^-(^1S_0) + Cl^+(^3P_2)$ channels are coupled enables one to determine the symmetry of the states involved in the diagram depicted in Fig. 4 (bottom). Correlation rules imply that a single ungerade state, of 0_u^+ symmetry [using Hund's case (c) notation], is associated with the $Cl^-(^1S_0) + Cl^+(^3P_0)$ limit, whereas two states of 0_u^- and 1_u symmetry correlate asymptotically to the $Cl^-(^1S_0) + Cl^+(^3P_1)$ limit and three states of 0_u^+, 1_u, and 2_u symmetry to the $Cl^-(^1S_0) + Cl^+(^3P_2)$ limit. Assuming that a homogeneous perturbation is responsible for the interactions, which is justified given that only the lowest rotational levels of Cl_2 are populated at the low temperature of the supersonic expansion (see also discussion in Refs. [18,19]), leads to the conclusion that the two Rydberg states and the ion-pair states are of 0_u^+ symmetry at short range and are thus accessible from the ground state in parallel electric-dipole transitions.

IV. CONCLUSIONS

The forced predissociation of ion-pair states of Cl_2 with effective principal quantum number $n^* = 1858$–1876 converging to the $Cl^-(^1S_0) + Cl^+(^3P_0)$ dissociation threshold into the $Cl^-(^1S_0) + Cl^+(^3P_2)$ ion-pair dissociation channel has been observed. The comparison of Cl^+, Cl^-, and Cl_2^+ ion yields enabled a qualitative analysis of the complex set of interactions between the accessible ionization and dissociation channels. A theoretical treatment based on close-coupled equations and channel elimination to calculate the nonadiabatic nuclear dynamics along the lines described in Ref. [31] would be very desirable to reach a quantitatively accurate understanding of the spectra.

From the value of the adiabatic ionization energy of the $X \rightarrow X^+$ transition in Cl_2 determined by pulsed-field ionization zero-kinetic-energy photoelectron spectroscopy [$E_I(Cl_2) = 92\,645.9 \pm 1.0\,cm^{-1}$ [17]], the known atomic ionization energy $Cl(^2P_{3/2}) \rightarrow Cl^+(^3P_2) + e^-$ [$E_I(Cl) = 104\,591.0 \pm 0.3\,cm^{-1}$ [23]] and the electron affinity of $Cl(^2P_{3/2})$ [$E_A(Cl) = 29\,138.6 \pm 0.4\,cm^{-1}$ [32]], the bond dissociation energies of $Cl_2(X\,^1\Sigma_g^+)$ and $Cl_2^+(X^+\,^2\Pi_u)$ can be determined to be

$$D_0(Cl_2) = E_{IPD}(^1S_0 + {}^3P_2) + E_A(Cl) - E_I(Cl) = 19\,998.4 \pm 1.1\,cm^{-1}, \quad (9)$$

$$D_0(Cl_2^+) = E_{IPD}(^1S_0 + {}^3P_2) + E_A(Cl) - E_I(Cl_2) = 31\,942.1 \pm 1.5\,cm^{-1}. \quad (10)$$

Compared with the latest results reported for these quantities [$D_0(Cl_2) = 19\,990^{+8}_{-2}\,cm^{-1}$, $D_0(Cl_2^+) = 31\,935^{+8}_{-2}\,cm^{-1}$ [17]], our results represent an improvement in precision by almost an order of magnitude.

ACKNOWLEDGMENTS

We thank A. Kirrander for making a preprint of Ref. [31] available prior to publication. This work is financially supported by the Swiss National Science Foundation (Project No. 200020-125030) and by the European Research Council (ERC Advanced Grant No. 228286).

[1] E. Reinhold and W. Ubachs, Mol. Phys. **103**, 1329 (2005).
[2] S.-H. Pan and F. H. Mies, J. Chem. Phys. **89**, 3096 (1988).
[3] A. G. Suits and J. W. Hepburn, Annu. Rev. Phys. Chem. **57**, 431 (2006).
[4] R. C. Shiell, X. Hu, Q. J. Hu, and J. W. Hepburn, Faraday Discuss. **115**, 331 (2000).
[5] J. D. D. Martin and J. W. Hepburn, Phys. Rev. Lett. **79**, 3154 (1997).
[6] M. O. Vieitez, T. I. Ivanov, E. Reinhold, C. A. de Lange, and W. Ubachs, J. Phys. Chem. A **113**, 13237 (2009).
[7] M. O. Vieitez, T. I. Ivanov, E. Reinhold, C. A. de Lange, and W. Ubachs, Phys. Rev. Lett. **101**, 163001 (2008).
[8] E. Reinhold and W. Ubachs, Phys. Rev. Lett. **88**, 013001 (2001).
[9] M. Cannon, C. H. Wang, F. B. Dunning, and C. O. Reinhold, J. Chem. Phys. **133**, 064301 (2010).
[10] W. A. Chupka, P. M. Dehmer, and W. T. Jivery, J. Chem. Phys. **63**, 3929 (1975).
[11] J. Berkowitz, C. A. Mayhew, and B. Ruscic, Chem. Phys. **123**, 317 (1988).
[12] T. Ridley, M. de Vries, K. P. Lawley, S. Wang, and R. J. Donovan, J. Chem. Phys. **117**, 7117 (2002).
[13] S. Wang, K. P. Lawley, and R. J. Donovan, Faraday Discuss. **115**, 345 (2000).
[14] T. Ridley, J. T. Hennessy, R. J. Donovan, K. P. Lawley, S. Wang, P. Brint, and E. Lane, J. Phys. Chem. A **112**, 7170 (2008).
[15] S. D. Peyerimhoff and R. J. Buenker, Chem. Phys. **57**, 279 (1981).
[16] D. B. Kokh, A. B. Alekseyev, and R. J. Buenker, J. Chem. Phys. **115**, 9298 (2001).
[17] J. Li, Y. Hao, C. Zhou, and Y. Mo, J. Chem. Phys. **127**, 104307 (2007).
[18] C. Zhou, Y. Hao, and Y. Mo, J. Phys. Chem. A **112**, 8263 (2008).
[19] Y. Hao, C. Zhou, and Y. Mo, J. Phys. Chem. A **113**, 2294 (2009).
[20] P. Rupper and F. Merkt, Rev. Sci. Instrum. **75**, 613 (2004).
[21] L. Zhu and P. Johnson, J. Chem. Phys. **94**, 5769 (1991).
[22] T. F. Gallagher, *Rydberg Atoms* (Cambridge University Press, Cambridge, 1994).
[23] J. E. Sansonetti and W. C. Martin, J. Phys. Chem. Ref. Data **34**, 1559 (2005).
[24] K. P. Huber and G. Herzberg, *Molecular Spectra and Molecular Structure*, Vol. IV, Constants of Diatomic Molecules (Van Nostrand Reinhold, New York, 1979).
[25] W. R. S. Garton, W. H. Parkinson, and E. M. Reeves, Proc. R. Soc. London **80**, 860 (1962).
[26] S. T. Pratt, E. F. McCormack, J. L. Dehmer, and P. M. Dehmer, Phys. Rev. Lett. **68**, 584 (1992).
[27] F. Merkt and T. P. Softley, Phys. Rev. A **46**, 302 (1992).
[28] F. Merkt and T. P. Softley, Int. Rev. Phys. Chem. **12**, 205 (1993).
[29] U. Fano, Phys. Rev. **124**, 1866 (1961).
[30] C. H. Greene and C. Jungen, Adv. At. Mol. Phys. **21**, 51 (1985).
[31] A. Kirrander (accepted by J. Chem. Phys.).
[32] U. Berzinsh, M. Gustafsson, D. Hanstorp, A. Klinkmüller, U. Ljungblad, and A.-M. Mårtensson-Pendrill, Phys. Rev. A **51**, 231 (1995).